Journal of Sound and Vibration (2003) **259**(5), 1199–1207
doi:10.1006/jsvi.2002.5201, available online at http://www.idealibrary.com on IDEAL®

A QUANTITATIVE EVALUATION OF ELASTIC WAVE IN SOLID BY STROBOSCOPIC PHOTOELASTICITY

Y.-H. Nam and S. S. Lee

Nondestructive Measurement group, Korea Institute of Standard and Science, Taejon 305-600, South Korea

(*Received* 28 *August* 2001, *and in final form* 28 *January* 2002)

We have developed a method for visually measuring and evaluating stresses emitted from an ultrasonic probe into a model solid similar to the actual material, by using image-processing techniques and stroboscopic photoelasticity. The visualization of wave stress (sound pressure) distribution can be achieved by synthesizing two photoelastic pictures, in which the directions of the principal axes of linear polariscopes are different by 45 degrees. The sound pressure field generated by commercial ultrasonic probes was measured by using the proposed method.

1. INTRODUCTION

There are many applications of a method for visually measuring and evaluating the ultrasonic wave emitted from a probe in the field of ultrasonic non-destructive testing: as a means of checking and improving ultrasonic probes, to aid ultrasonic testing of components of a complex shape, to study the basic behavior of ultrasonic pulses, as a tool for training ultrasonic operators, etc. [1–6].

Some conventional photoelastic methods for the visualization and evaluation of ultrasonic stress waves (the sound pressure) use a circular polariscope, and a stroboscopic light source with a very short flashing time obtains a still picture of the ultrasonic wave travelling at high speed. No detailed quantitative measurement has yet been successful because of the low sensitivity for the sound pressure analysis [7, 8].

This paper presents a new method of experimental analysis of the wave stress field based on the synthesized technique of photoelastic pictures. In the synthesized picture, the brightness at any point depends on the principal stress difference at that point, and the wave stress can be evaluated quantitatively by measuring the intensity on the synthesized picture. Synthesized pictures were obtained by synthesizing two pictures in which the principal axes of a crossed linear polarizer are different by 45°, using a linear polarization type of photoelastic apparatus with stroboscope light source [9–12]. This paper describes the principle of this method and the results of several measurements.

2. DESCRIPTION OF THE SYSTEM

The components of the system developed in this study are diagrammed in Figure 1. The system consists of a regular linear polariscope with a commercial stroboscopic light source and a digital image-processing system for the photoelastic stress analysis. The ultrasonic testing system, whose rate of repetition and synchronized output is 60 Hz, drives the

0022-460X/02/$35.00

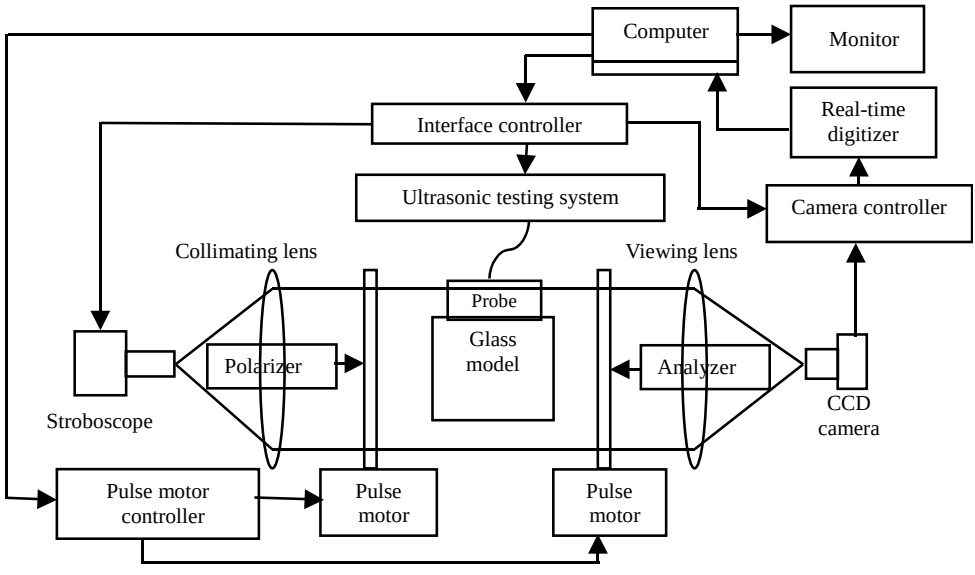

Figure 1. Diagram of the visualization and evaluation system.

ultrasonic probe to generate pulsed ultrasonic waves into the test piece, as is similar to that of the ultrasonic non-destructive testing. A commercial stroboscope light source, giving a light flashing of a very short duration (less than 200 ns), is positioned at the focal point of a collimating lens, whose effective diameter of field is 150 mm.Trigger pulses are sent from the interface controller to stroboscope, ultrasonic testing system and TV camera controller for their synchronization with each other. The trigger pulse actuating the stroboscope has the delay time to the trigger pulse of an ultrasonic testing system, and by varying this delay time an observer can change the position at which the pulsed ultrasonic wave is stroboscopically "frozen" and imaged.

All of the visualized images are obtained using Pyrex glass of 20 mm thickness. There are three reasons why Pyrex glass was used as a test piece. First, the ultrasonic wave velocities of this glass (longitudinal wave velocity: 5490 m/s; shear wave velocity: 3420 m/s) are similar to those of steel, so that the angle probe for the emission of refracted shear wave can be used to simulate the practical angle beam testing. Second, it has a better optical coefficient than most inorganic glasses. Third, the attenuation of ultrasonic waves in it is less than in other photoelastic materials such as an epoxy resin.

Two visualized images with 45° different polarizer orientations are synthesized in the image-processing computer or conventional 35 mm camera, using the double-exposure technique in this case, to avoid the variation of visualized sensitivity with wave propagation direction relative to the orientation of incident polarized light. A TV camera uses a special high-sensitivity vidicon television-camera tube to visualize the ultrasonic wave in solid. The picture is divided into 512 lines and each line is divided into 512 parts. The brightness is converted into a video signal with 8-bit resolution. A monitor displays the information and acts as a graphics/numeric terminal for image processing, wave stress data analysis, program development, and graphical data display. A computer has a 16-bit CPU and special hardware for image processing to perform the sound pressure analysis within a short time.

3. SYNTHESIZED PHOTOELASTIC PICTURE METHOD

Figure 2 explains the brightness at any point when the same stress field is observed in the linearly polarized lights. In the figure, the intensity of brightness at any point on the first picture is I_1 and on the second picture is I_2.

In the case of image taken under the condition of (a),

$$I_1 = a^2 \sin^2 2\theta \sin^2 \frac{\delta}{2}. \tag{1}$$

In the case of image taken under the condition of (b),

$$I_2 = a^2 \cos^2 2\theta \sin^2 \frac{\delta}{2}, \tag{2}$$

$$\delta = cd(\sigma_1 - \sigma_2).$$

where σ_1, σ_2 are the principal stress values, c is the Photoelastic constant, d is the thickness of test piece, and θ is the angle between the direction of σ_1 and the principal axis of polarizer in the first picture.

In the case of a synthesized picture in which the intensity of brightness of the first picture is added to that of the second picture, the intensity of brightness at any point corresponds to only the principal stress difference, so that the relationship between the intensity of brightness and the principal stress difference is the same as the case of circular polarization.

Synthesized picture:

$$I = I_1 + I_2 = a^2 \sin^2 \frac{\delta}{2}. \tag{3}$$

Since the relationship between the principal stress components is known in the case of ultrasonic longitudinal wave and shear wave as shown in Figure 2, the ultrasonic wave stress (sound pressure) can be measured and evaluated at any point by measuring the intensity of the brightness on the synthesized picture [13–16].

In the case of sound pressure to longitudinal wave:

$$\sigma_1(\sigma_2 = 0). \tag{4}$$

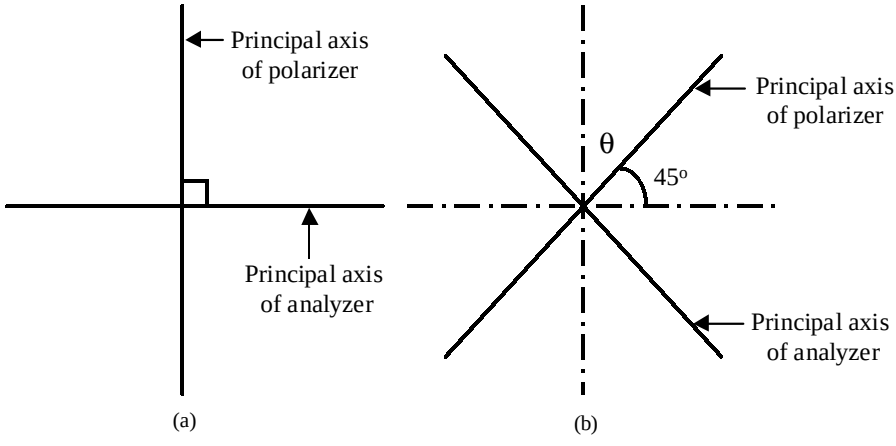

Figure 2. Synthesized photoelastic method.

In the case of sound pressure to shear wave:

$$\sigma_1(\sigma_2 = -\sigma_1). \tag{5}$$

Figure 3 illustrates the determination of wave phase using the photoelastic method. Since the ultrasonic wave is stroboscopically frozen and imaged, the visualized stress field of the ultrasonic wave is treated as a static stress field condition. Figure 3(a) schematically represents the visualized longitudinal wave emitted from a normal longitudinal probe and the relationship between the wave stress and the intensity of the visualized image along the A–B line. As shown, only absolute values of wave stress at any point on the ultrasonic wave are obtained by measuring the intensity of the brightness at these points. When small and static compressional stress is applied parallel to the direction of the travel of the longitudinal wave, for example, by pushing the probe on the test piece by hand, applied compressional stress is added to that of wave stress. Since the intensity of the brightness corresponds to the absolute values of total stress at that point, the intensity in the compression phase of the longitudinal wave is increased and the intensity in the tension phase is decreased because of the application of the compressional stress as shown in Figure 3(b). The wave phase in the longitudinal wave can be determined from the change of the intensity of the brightness on the visualized wave when applying the static compressional stress.

Figure 4 also illustrates the determination of the wave phase in the case of shear wave. Since the direction of principal stress in shear wave is different by 45° from the direction of travel of shear wave, a static compressional stress has to be applied parallel to the direction of the principal stress axis for the determination of wave phase to be possible. As in the

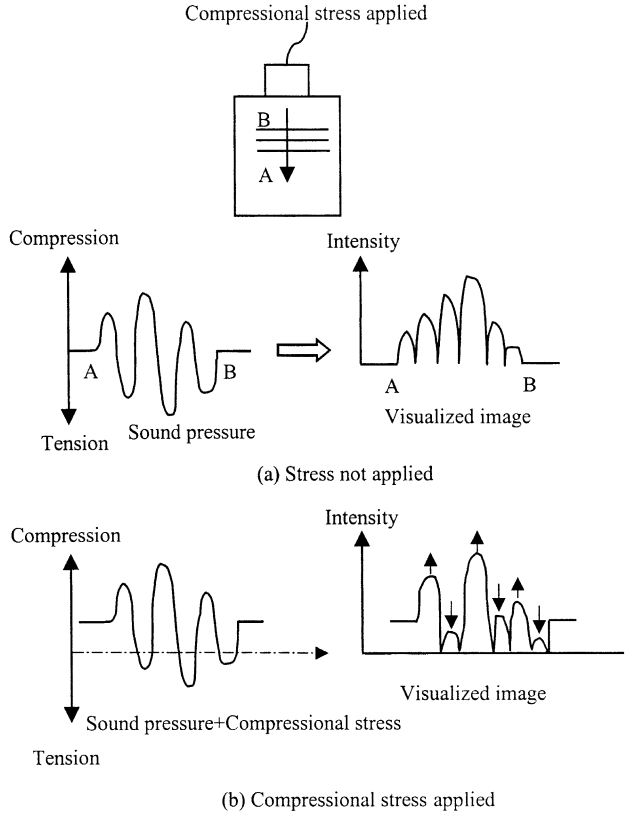

Figure 3. Determination of wave phase in longitudinal wave.

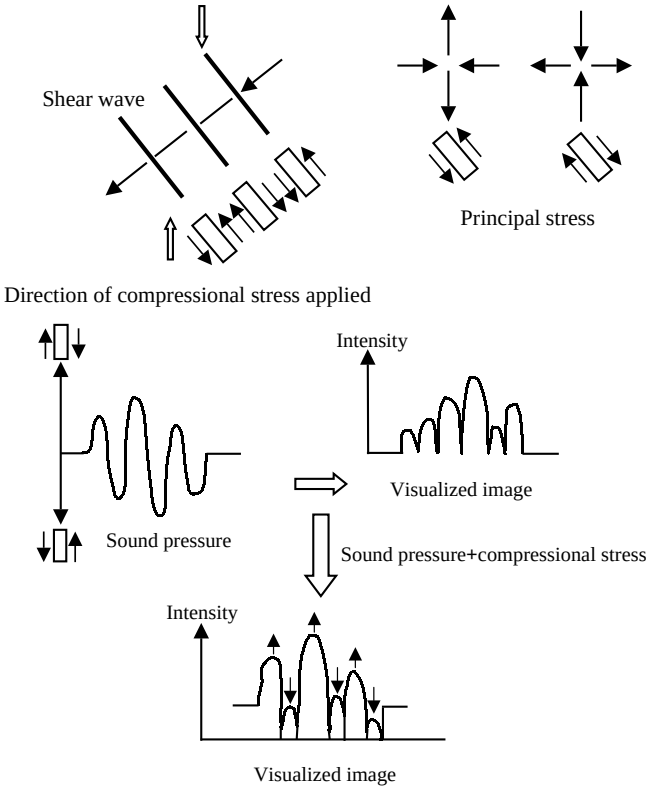

Figure 4. Determination of wave phase in shear wave.

case of longitudinal wave, the phase of shear wave can be determined by the change of intensity on the visualized shear wave when compressional stress is applied, as shown in Figure 4.

4. SOUND PRESSURE MEASUREMENT

A calibration curve between the intensity of the brightness on the synthesized picture and the stress value, which is equal to the sound pressure value, is obtained by providing the synthesized picture with an application of a concentrated load of known magnitude to the glass test piece. Intensity distribution is converted to sound pressure distribution using this calibration curve in the computer.

Figure 5 shows the visualized image of ultrasonic shear wave from an angle probe, obtained by the synthesized photoelastic method. The frequency and nominal refraction angle of the angle probe are 2 MHz and 45° respectively.

Figure 6 shows a three-dimensional image of the sound pressure distribution of the shear wave field in Figure 5.

Figure 7 shows the relationship between the distribution of sound pressure and the change of intensity distribution along the centerline of the visualized longitudinal wave parallel to the direction of wave travelling.

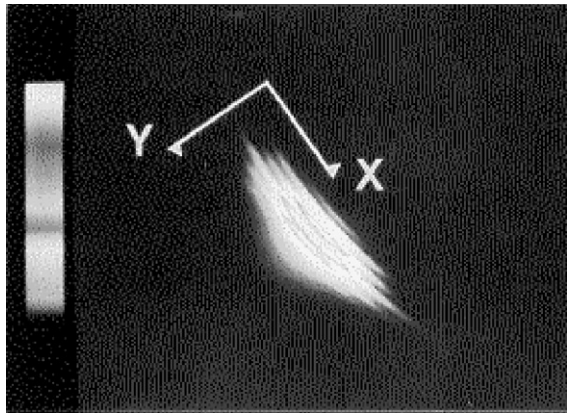

Figure 5. Visualized shear wave.

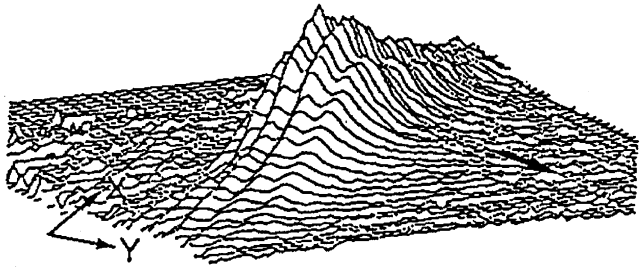

Figure 6. Three-dimensional image of sound pressure distribution in shear wave.

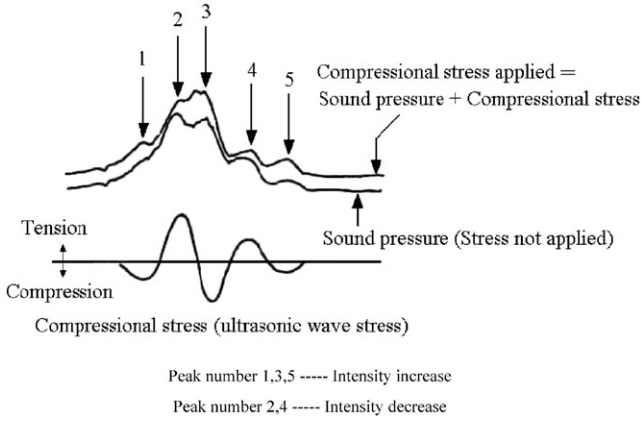

Figure 7. Change of intensity and its relation to phase of wave.

Figure 8 shows a sound pressure distribution on the centerline of the longitudinal wave in the direction of wave travelling.

Figure 9 also presents the change of intensity distribution in the centerline of shear wave by applying the static compressional stress to determine the wave phase. As is apparent from this figure, the intensity decreases and increases on the visualized wave occur

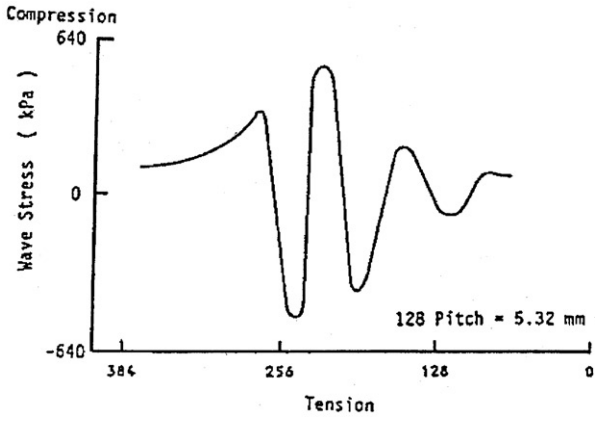

Figure 8. Wave stress distribution in longitudinal wave.

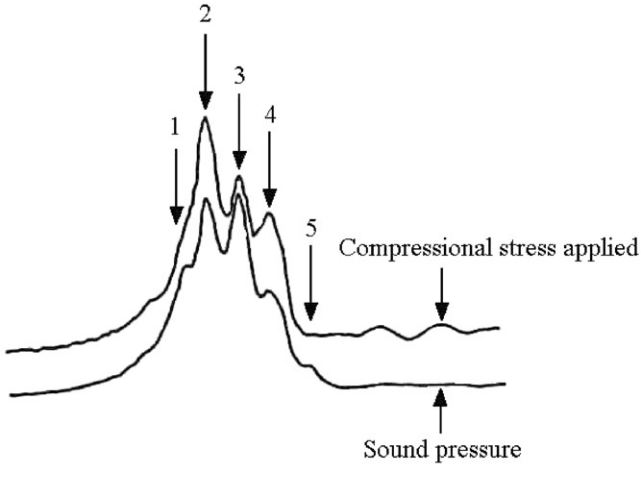

Peak number 1, 3, 5 ----- Intensity decrease

Peak number 2,4 ----- Intensity increase

Figure 9. Change of intensity in shear wave.

alternatively as mentioned in Figures 3 and 4. The phase of ultrasonic wave can be determined from these results.

Figure 10 shows a sound pressure distribution in the centerline of shear wave in the travelling direction.

Figure 11 presents typical examples of scattering of ultrasonic waves at a cylindrical hole. In the case of shear wave, incident shear wave (A) to a 3 mm diameter cylindrical hole produced two reflected shear waves (C, D) and mode-converted longitudinal wave (B). The second reflected shear wave (D) is accompanied by the surface wave propagating along the cylindrical hole that is mode-converted from the incident shear wave at the reflection of the hole. As shown in this figure, an important feature of ultrasonic wave behavior in solids is the effect of reflection and mode-conversion at the defect surface. This feature is strikingly evident when using this ultrasonic visualization method.

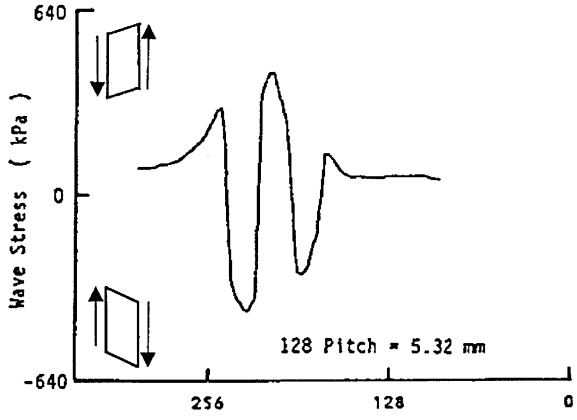

Figure 10. Wave stress distribution in shear wave.

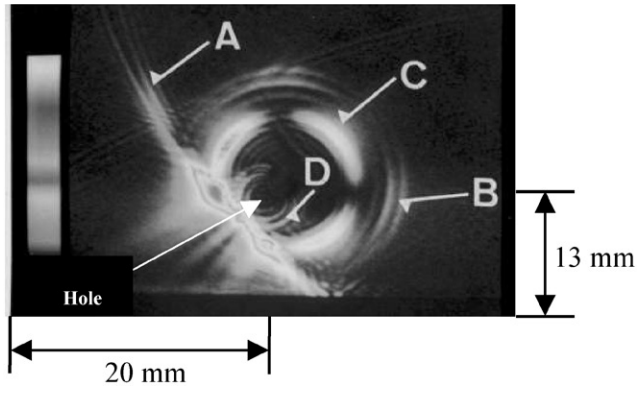

Figure 11. Reflection of shear wave from a 3 mm diameter cylindrical hole.

5. CONCLUSION

This paper describes a synthesized photoelastic method developed for the visualization and evaluation of sound pressure distribution of ultrasonic wave in a solid. The visualization of wave stress field is achieved by synthesizing two photoelastic pictures, in which the direction of the principal axis of linear polariscopes differs by 45°. From the analysis of the wave stress distribution using this method, it is possible to evaluate the characteristics of ultrasonic waves in a solid, such as the intensity of stress, directivity and resolution characteristics of the wave emitted from a commercial probe, and characteristics of scattering from various types of defects.

REFERENCES

1. K. G. Hall 1976 *Non-destructive Testing* 121–126. Crack depth measurement in rail steel by Raleigh waves aided by photoelastic visualization.
2. K. G. Hall 1977 *Ultrasonics* **15**, 245–252. A qualitative evaluation of variable-angle ultrasonic transducers by the photoelastic visualization method.

3. J. A. Archer-Hall and D. A. Hutchins 1979 *Ultrasonics* **17**, 209–212. The photoelastic visualization of ultrasonic waves in liquids.
4. K. G. Hall 1982 *Ultrasonics* **20**, 159–170. Observing ultrasonic wave propagation by stroboscopic visualization methods.
5. G. M. Light, A. Singh and T. Rudwick 1982 *Materials Evaluation* **40**, 783–790. Ultrasonic transducer characterization using the combined schlieren, photoelastic, and Raman Nath (SPRN) system.
6. Y. Bar-Cohen 1983 *Materials Evaluation* **41**, 88–93. Schlieren visualization of acoustically imaged defects.
7. K. G. Hall 1984 *British Journal of NDT*, 162–171. Railway applications of ultrasonic wave visualization techniques.
8. K. G. Hall 1984 *Materials Evaluation* **42**, 922–929. Visualization techniques for the study of ultrasonic wave propagation in the railway industry.
9. S. Y. Zhang, J. Z. Shen and C. F. Ying 1988 *Materials Evaluation* **46**, 638–641. The reflection of the Lamb wave by a free plate edge: visualization and theory.
10. C. W. Hennige 1989 *Materials Evaluation* **47**, 496–499. Schlieren optical system for visualizing ultrasonic waves.
11. A. McNab and I. H. Cornwell 1995 *Insight* **37**, 814–819. Visualization of 3D ultrasonic NDT data.
12. M. N. Rychagov and H. Ermert 1996 *Ultrasonics* **34**, 517–522. Cross-flow visualization by acoustic CT measurements.
13. K. Date and Y. Udagawa 1989 *Review of Progress in Quantitative Nondestructive Evaluation* **8B**, 1755–1762. Visualization of ultrasonic waves in a solid by stroboscopic photoelasticity and image processing techniques.
14. Y. H. Nam 1999 *KSME International Journal* **13**, 158–167. Directivity analysis of ultrasonic waves on surface defects using a visualization method.
15. Y. H. Nam 1999 *Welding Journal* **78**, 338–342. Directivity evaluation of an artificial defect in a simulated butt joint by the visualization method.
16. Y. H. Nam 2001 *KSME International Journal* **15**, 441–447. Modeling of ultrasonic testing in butt joint by ray tracing.